Al-Nahrain Journal of Science
ANJS, Vol.26(4), December 2023, pp. 73-79

Synthesis and Characterization of ZrO_2:ZnO Nanoparticles Prepared by Laser Induced Plasma

Marwa A. Mohammed[1,*], Hassan Hashim[2]

[1,2] Department of Physics, College of Science, Al-Nahrain University, Baghdad, Iraq.

Article's Information

Received: 10.07.2023
Accepted: 29.10.2023
Published: 01.12.2023

Keywords:
Laser induced Plasma
ZrO_2:ZnO
XRD
AFM
UV-VIS spectroscopy

Abstract

In this research, we looked at how laser energy affected the structural and optical characteristics of ZrO_2:ZnO thin films at mixing ratios (0.1, 0.2, 0.3 and 0.4) that were applied on glass slides using the pulse laser deposition technique (PLD). Nd:YAG laser was utilized with a wavelength of 1064 nm, a pulse width of 9 ns, and an energy of 320 mJ. The X-ray diffraction patterns revealed that all the films had a polycrystalline hexagonal crystal structure. AFM was used to measure the topography of the film's surface, and the results revealed that the average roughness and grain size increased. After analyzing the optical characteristics of each film, it was discovered that the absorption coefficient in the 200–1000 nm wavelength range increases at 320 mJ of laser energy and that the optical energy gap value for indirect permitted transitions decreases between 3.58 and 3.4 eV.

DOI: 10.22401/ANJS.26.4.11

*Corresponding author: st.marwa.ahmed@ced.nahrainuniv.edu.iq

1. Introduction

In 1960, one of the best and most cheap techniques for producing oxides, deposits of minerals, and semiconductors in a variety of technical applications was pulse laser deposition [1]. Since late 1987, when T. Venkatesan and coworkers—one of the authors of this issue—discovered that the extreme nonequilibrium conditions produced by pulsed laser melting of YBaCuO permitted the in-situ formation of thin films of this high transition temperature (T_c) superconducting material, research on materials grown by pulsed laser deposition, or PLD, has seen phenomenal growth. Since then, PLD has become the main method for producing high-quality superconducting thin films in large quantities for use in devices and research[2]. Thin films of conductive oxide (TCO), like zinc oxide [3], have low resistance and excellent optical transmittance. ZnO is a semiconductor material with several uses due to its large and direct energy gap of 3.3 eV, which is close to the UV area. Numerous opto-electronic applications of ZnO may be found in solar cells, spintronics [4], [5], laser diodes (LDs), and light-emitting diodes (LEDs)[6]. Due to internal structural faults like oxygen and zinc gaps, or interstitial conditions in a lattice, ZnO is an n-type semiconductor material [7]. ZnO nanostructured thin films have been produced using a variety of methods, including thermal evaporation[8], magnetron sputtering [8], sputtering[9], chemical vapor [10], and ion-beam assisted [11]. The laser-induced plasma (LIP) approach is one of the most popular and alluring methods for creating nanostructured thin films with a particular property [12]. Metal oxide materials can be generated as high-quality nanofilms utilizing the laser-induced plasma (LIP) process .The benefit of LIP over their techniques is that multilayered films made of various materials may be produced very easily.Although zirconium oxide has numerous applications, large band gap metal oxide nanoparticles have caught the interest of scientists. Due to its superior chemical and physical qualities, zirconium oxide (ZrO_2), commonly known as zirconia, is used in a variety of products, including fuel cells [15], gas sensors [16], optoelectronics, catalysts , and corrosion-resistant materials [19]. ZrO_2 has a band gap of 5 eV and is a significant luminous material with

good optical transparency . Its high surface area and abundance of oxygen vacancies make it a possible option for photocatalytic applications [21].ZrO_2 nanostructures can be made using a variety of techniques, including sol-gel[22], hydrothermal [23], combustion [24], and co-precipitation [25,26].

2. Experimental Details:

The four ZrO_2:ZnO nanostructure samples in the current work are precipitated on glass using micro-powders of zinc oxide and zirconium oxide that are accessible and have a purity of 99.99%. Zirconium oxide powder and zinc powder were mixed in a variety of weight ratios according to the following formula:

$$WZrO_2 + ZnO \rightarrow WZrO_2(x) + WZnO(1-x) \quad \ldots(1)$$

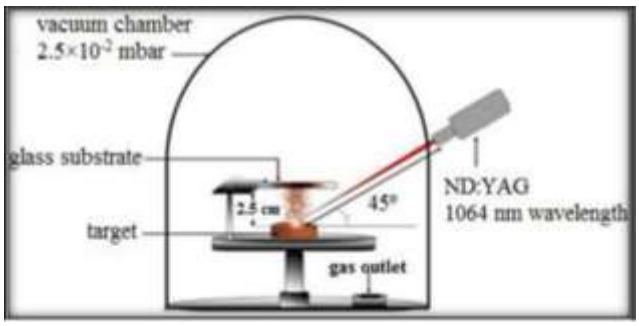

Figure 1: Schematic representation of a system for pulsed laser deposition

The results for Mixing between ZrO_2 & ZnO ($W_{ZrO2 + ZnO}$ = 2gm), (0.22 from zirconium oxide and 1.77 from zinc oxide were mixed for a ratio of 0.1; than 0.43 from zirconium oxide and 1.56 from zinc oxide were mixed for a ratio of 0.2). A weight ratio of 0.64 from zirconium oxide and 1.35 from zinc oxide were mixed for a ratio of 0.3; than 0.85 from zirconium oxide and 1.14 from zinc oxide were mixed for a ratio of 0.4. The substrates were positioned inside the chamber with a 10 cm gap between them and the target, and then a steady 150 watt power source was used during the two-hour deposition procedure. A basic vacuum pressure of 10^{-5} bars was used within the chamber to conduct the deposition operation. PLD was used in this work to deposit (ZrO_2:ZnO) films. By aiming the laser at the target (the pellet), which causes the material to evaporate and grow on the substrate, thin film growth was accomplished. The Nd:YAG laser, which has a wavelength of 1064 nm, was utilized for the growth process of films. The duration and energy of the laser pulses, among other laser parameters, affect the evaporation process [27]. The experiment was carried out in a vacuum chamber at a pressure of 2.5×10^{-2} mbar. Using a hydraulic piston of the SPECAC type, the (ZrO_2:ZnO) target was created using 6 Pa of pressure over the course of 10 minutes, yielding a disc with a (2.5 cm) diameter and (200 nm) thickness. This research examined the structural and morphological characteristics of thin films made of ZrO_2:ZnO on glass slides. Nd:YAG laser with 200 pulses per shot, 320 mJ of energy, (f = 6Hz) of frequency, and 1064 nm wavelength (**λ**). The angle formed by the incident Nd:YAG SHG Q-switching laser beam and the target surface is approximately 45 degrees. As shown in Fig. 1, the first vacuum system is a rotating vacuum system with two stages, a pressure and temperature gauge, and a vacuum chamber. Through the use of X-ray diffraction (XRD) and atomic force microscopy (AFM), the crystal structure and morphology were investigated. To ascertain the films' optical characteristics, ultraviolet spectroscopy (UV) analysis was also performed.

3.Results and discussion:

3.1 - X-ray diffraction examination: The crystalline structure and grain size of the (ZrO_2:ZnO) films produced by PLD procedures were determined using X-ray diffraction (XRD). Through the use of Scherrer's equation, the grain size (D) was calculated [28][29];

$$D = \frac{K.\lambda}{\beta\, Cos(\theta_\beta)} \quad \ldots(2)$$

Where β full width at half maximum (FWHM), $\boldsymbol{\theta_\beta}$ Bragg's angle, and λ is X-ray wavelength (1.54 A°), where 0.94 is assumed to be a constant for k. The crystalline structure and grain size of the ZnO and ZrO_2 produced by PLD procedures were determined using X-ray diffraction (XRD). The use of the X-ray diffraction technique revealed that polycrystalline structures were used in the preparation of all thin films. The XRD patterns for ZnO powder are shown in Figure 2, which demonstrate the material's hexagonal structure and diffraction peaks at crystalline hkl (100), (002), (101), (102), (110), (103), (200), (112), and (201). This correspond to 2θ = 31.8°, 34.4°, 36.3°, 47.5°, 56.6°, 62.8°, 66.4°, 67.9° and 69.1°, and the average crystallite size is 39 nm. The outcomes are fairly consistent with the standard values of the supplied data (JCPDS No. 98-004-1488). Using

Scherrer's equation, the experimental inter-plane gap and crystal size were determined.
It may contain subheadings, which are divided into numbered subsections.

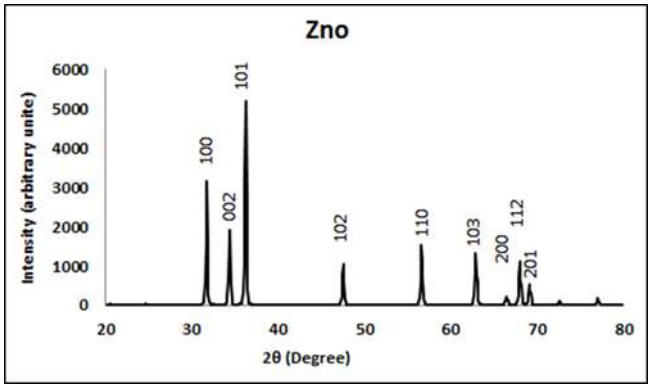

Figure2. X-ray pattern of ZnO Powder

While the XRD patterns for ZrO_2 powder are shown in Figure 3, which show that the material has a hexagonal structure with diffraction peaks at crystalline hkl (110), (002), (101), (012), (110), (113), (103), (112) and (201), which correspond to 2θ = 31.8º, 34.6º, 36.35º, 47.7º, 56.65º, 63.1º, 66.4º, and 68.1º, and the average crystallite size is 33 nm, the outcomes are quite consistent with the normative values of the supplied data (No. 98-008-8320).

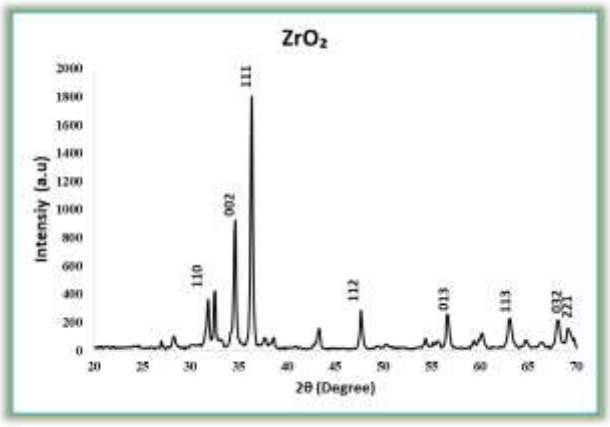

Figure 3. X-ray pattern of ZrO_2 Powder

Figure 4 shows the X-ray diffraction of thin ZrO_2:ZnO films that are 200 nm thick at X = 0.1, 0.2, 0.3, and 0.4. Peaks of the material (ZnO) with hkl [(100), (002), (101), (012), (110), (013), (112), and (201)] emerge at 2θ = 31.8º, 34.5º,36.3º,47.7º,56.75º,62.9º and 68.05º and peaks of the Zr with hkl [(111), (200), (202), (311)] and emerge at 2θ = 30.3º, 35.3º, 50.5º, 60.3º, and 63º and the average crystallite size for ZnO at (0.1, 0.2, 0.3 and 0.4) is 20.66 nm, 20.79 nm, 21.83, and 22.78 nm, and the average crystallite size for ZrO_2 with the same proportions is 21.10 nm and 22 nm, which are identical to JCPDS card No. (98-004-1488) for ZnO and card No. (98-0088320) for ZrO_2. Crystal development begins with a spike in doping. There is no doubt that crystallization is developing, and because there are numerous peaks and a hexagonal pattern, it appears that the sedimentary models have a polycrystalline structure. From Figure 4, we conclude that the average crystal size increases with increasing ZrO_2:ZnO ratios.

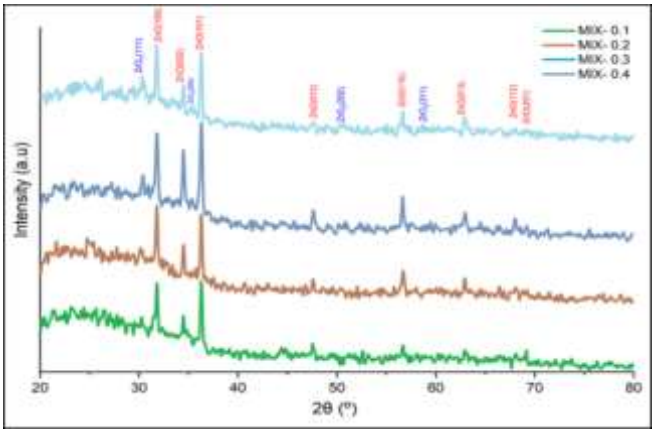

Figure 4. X-ray diffraction pattern for mix ZrO_2:ZnO

3.2 Atomic force microscopy:

Atomic force microscopy (AFM) was used to examine the surface morphology of the thin film that had been deposited. Figure 5 displays the acquired AFM images for both pure and doped thin films. The morphological characteristics of the deposited films can be predicted using image analysis; for example, the films may have grains of varying sizes, uneven forms, and separation. It can be concluded from a comparison of images taken at various zirconium oxide concentrations that the concentration of zirconium oxide significantly improved the morphological qualities of the films. When ZrO_2 doping ratios and grain sizes are raised, the roughness values and root mean square RMS rise, which causes the film's surface to become rough [[28],[29].

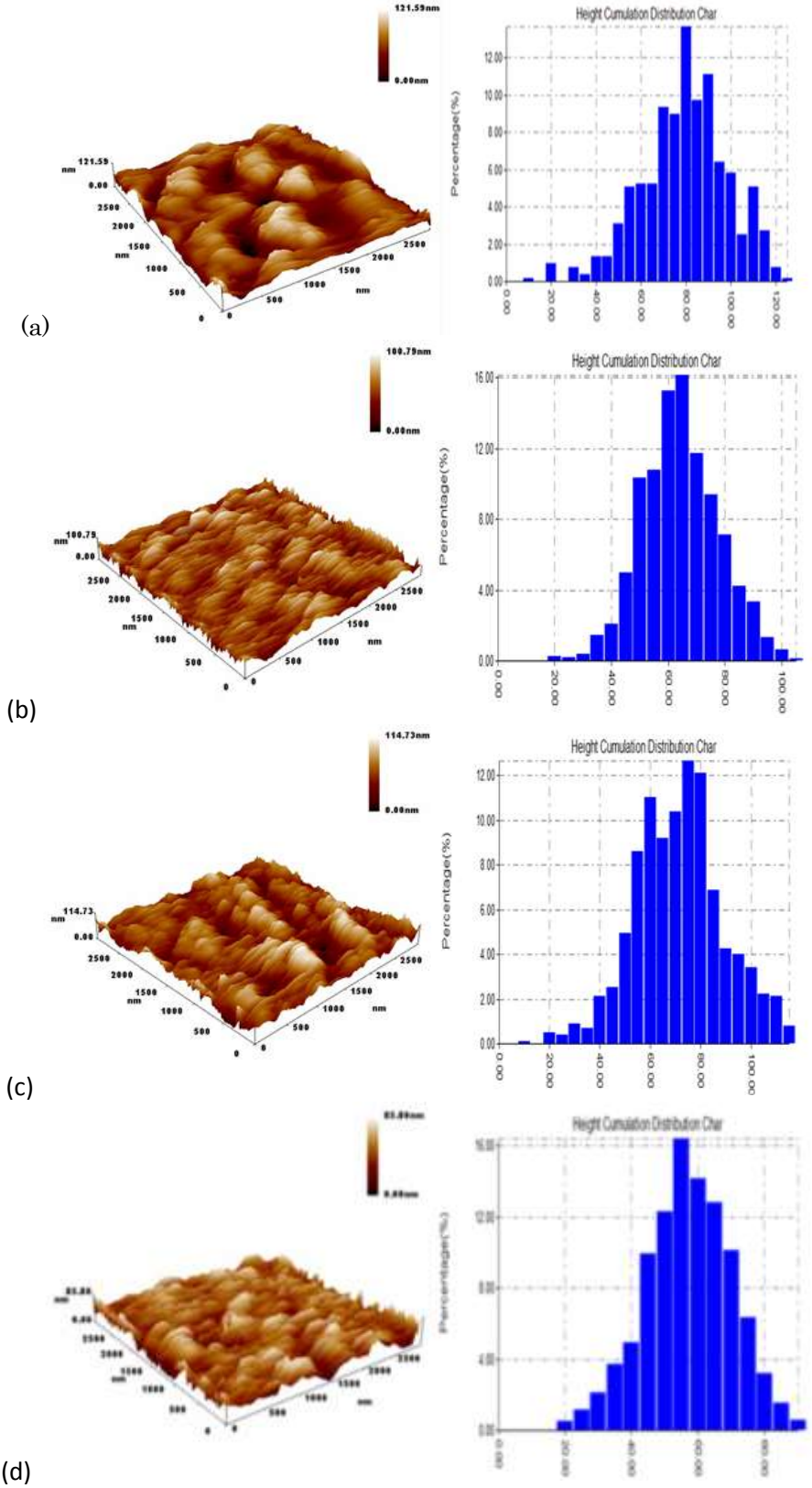

Figure 5. Images of ZrO_2: ZnO thin films deposited with different concentrations of (a) 0.1 (b) 0.2 (c) 0.3 and (d) 0.4.

The average diameter, root mean square, and average roughness of ZrO_2:ZnO thin films are shown in Table 4 as AFM parameters. Laser pulses were used to deposit the thin layers on the glass substrate.

Table 1. The average roughness, root mean square, and average grain size for ZrO_2:ZnO thin films.

Sample	Ratio	Avg. Diameter (nm)	Root Mean Sq. (nm)	Avg. Roughness (nm)
ZrO_2:ZnO	0.1	74.04	13.5	10.1
	0.2	78.7	14.4	11.3
	0.3	89.06	17.9	14.4
	0.4	91.61	20.6	16.4

3.3 The absorption coefficient:

An UV-Vis spectrophotometer with a double beam was used to determine the optical characteristics. Taiwan's (MetertechSP8001). Tauc's formula for direct transition was used to graphically estimate the optical band gap [30].

$$\alpha h\nu \propto (h\nu - E_g)^n \quad \ldots(3)$$

$$(\alpha h\nu)^2 \propto A(h\nu - E_g)^n \quad \ldots(4)$$

where α is the absorption coefficient, h is the Planck constant, ν is the frequency of the photon, E_g is the optical energy gap, and n is a constant that is dependent on the nature of the transition. A is a constant that relies on the nature of the material. PLD, or pulse laser deposition, was employed. At laser energy E = 320 mJ, the absorption coefficient (α) varies as a function of wavelength in all films of Zinc oxide doped with Zirconium Oxide ZrO_2:ZnO (X = 0.1, 0.2, 0.3 and 0.4), as shown in Figure 6. According to the findings, raising the doping ratio caused all absorption coefficient values for the state reconstitution to increase significantly. Considering that donor levels are produced in the energy gap just outside the conduction band [30].

3.4 Calculation of the optical energy gap (Eg):

The amount to which thin films produced during the production of hybrid joints, reagents, and solar cells may be used depends critically on the optical energy gap. In the event, a diagram illustrating the link was plotted as a function of photon energy ($h\nu$), as seen in Figure 7, where the intersection of the straight portion of the curve with the photon energy axis $(\alpha h\nu)^2 = 0$) represents the magnitude of the direct visual energy gap. Figure 7 displays the optical energy gap for the direct ZrO_2:ZnO film transport that is permitted as well as the optical energy gap for indirect ZrO_2:ZnO films' permissible transport at X = 0.1, 0.2, 0.3, and 0.4.

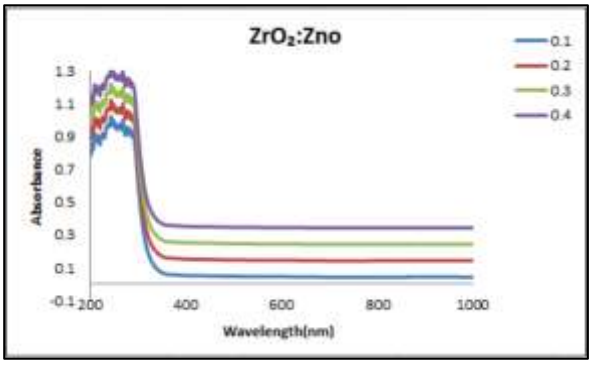

Figure 6. The absorption coefficient for pure ZrO2:ZnO (X =0.1, 0.2, 0.3, and 0.4) varies with wavelength.

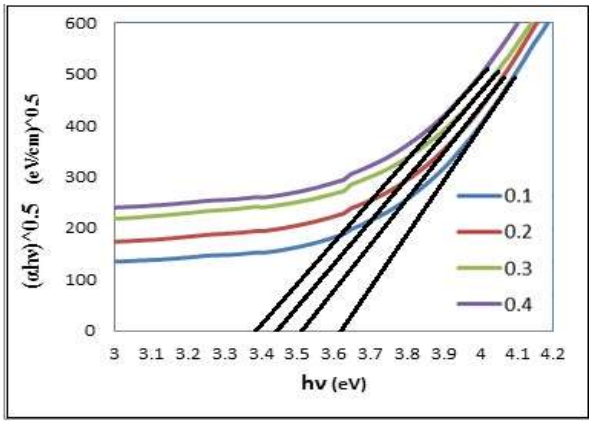

Figure 7. The dependence of $(\alpha h\nu)^{1/2}$ on photon energy ($h\nu$) for ZrO_2:ZnO thin films produced on glass substrates.

The results show that the energy gap is an indirect allowed gap, and the value of the absorption coefficient is equal to $\alpha > 10^4$, demonstrating that the energy gap is 2.0 eV for the permitted indirect transmission of a membrane (ZrO_2:ZnO). This conclusion is consistent with the findings of earlier studies. The decrease in the optical bandgap is caused by an increase in ZrO_2:ZnO composition in various preparation methods. According to Mohammed et al. (2022)[31], the aggregation in the samples might have been responsible for the redshift and decrease of the band gap energy. Table 2 lists all values in tabular form.

Table 2. The energy gap of ZrO_2:ZnO for (X=0.1,0.2 ,0.3and 0.4) deposited.

Sample (X mixing ratio)	E_g (eV)
0.1	3.58
0.2	3.5
0.3	3.46
0.4	3.4

3.5 Conclusions

The ZrO_2:ZnO the film was prepared using an Nd:YAG laser with a fundamental wavelength of 1064 nm. on the glass substrate. The X-ray findings revealed that all thin films are polycrystalline and have a hexagonal structure with direction dominance (111). The results of AFM show that the higher the percentage of doping, the increase in grain size. As for the properties measurements, it was found that the absorption coefficient increase as the percentage of doping increases. Whereas the energy gap, on the other hand, decreases with the rate of doping increases.

References:

[1] Ashfold, M.N.R.; Claeyssens, F.; Fuge, G.M.; Henley, S.J.; "Pulsed laser ablation and deposition of thin films". Chem. Soc. Rev., **33**(1): 23–31, 2004.

[2] Hubler, G.K.; "Pulsed laser deposition". MRS Bull., **17**: 26–29, 1992.

[3] Aksoy, S.; Caglar, Y.; Ilican, S.; Caglar, M.; "Effect of heat treatment on physical properties of CdO films deposited by sol–gel method". Int. J. Hydrogen Energy, 34(12): 5191–5195, 2009.

[4] Srinatha, N.; Raghu, P.; Mahesh, H. M.; Angadi, B.; "Spin-coated Al-doped ZnO thin films for optical applications: Structural, micro-structural, optical and luminescence studies". J. Alloys Compd., 722: 888–895, 2017.

[5] Hasabeldaim , E.; Ntwaeaborwa, O. M.; Kroon, R. E.; Coetsee, E.; Swart, H. C.;"Effect of substrate temperature and post annealing temperature on ZnO: Zn PLD thin film properties". Opt. Mater. (Amst). 74: 139–149, 2017.

[6] Mustafa, S. K.; Jamal, R. K.; Aadim, K. A.; "Studying the effect of annealing on optical and structure properties of ZnO nanostructure prepared by laser induced plasma" Iraqi J. Sci.,60(10): 2168–2176, 2019.

[7] Shan, F. K.; Shin, B. C.; Jang, S. W.; Yu, Y. S.; "Substrate effects of ZnO thin films prepared by PLD technique". J. Eur. Ceram. Soc., 24(6): 1015–1018, 2004.

[8] Mani, G. K.; Rayappan, J. B. B.; "A highly selective and wide range ammonia sensor—Nanostructured ZnO: Co thin film". Mater. Sci. Eng. B, 191: 41–50, 2015.

[9] Larbah, Y.; Adnane, M.; Sahraoui, T.; "Effect of substrate temperature on structural and optical properties of spray deposited ZnO thin films". Mater. Sci., 33(3): 491–496, 2015.

[10] Shan, F. K.; Yu, Y. S.; "Band gap energy of pure and Al-doped ZnO thin films". J. Eur. Ceram. Soc., 24(6): 1869–1872, 2004.

[11] Craciun, V.; Elders, J.; Gardeniers, J. G. E.; Boyd, I. W.; "Characteristics of high quality ZnO thin films deposited by pulsed laser deposition". Appl. Phys. Lett., 65(23): 2963–2965, 1994.

[12] Vanalakar, S. A.; Agawane, G.L.; Shin, S.W. ; Suryawanshi, M.; Gurav, K.V.; Patil, P.S.; Jeong, C.; Kim, J.Y.S.; Kim, J.H.; "A review on pulsed laser deposited CZTS thin films for solar cell applications". J. Alloys Compd., 619: 109–121, 2015.

[13] Fan, X. M.; Lia, J. S.; Guo, Z. X.; Lu, H. J.; "Microstructure and photoluminescence properties of ZnO thin films grown by PLD on Si (1 1 1) substrates"; Appl. Surf. Sci., 239(2), pp. 176–181, 2005.

[14] Kumar, V.; Ntwaeaborwa, O. M.; Swart, H. C.; "Deep level defect correlated emission and Si diffusion in ZnO: Tb3+ thin films prepared by pulsed laser deposition"; J. Colloid Interface Sci., 465: 295–303, 2016.

[15] Horti, N. C.; Kamatagi, M. D.; Nataraj,S. K.; Wari , M. N.; Inamdar, S. R.; "Structural and optical properties of zirconium oxide (ZrO2) nanoparticles: effect of calcination temperature". Nano Express, 1(1): 10022, 2020.

[16] Rossall, A. K., "Characterisation and Measurement of Laser Produced Plasma

Emission and Applications in Opacity Experiments". PhD. Thesis. University of York. 2011.

[17] Wang, X.; Zhai, B.; Yang, M.; Han, W.; Shao, X.; "ZrO2/CeO2 nanocomposite: Two step synthesis, microstructure, and visible-light photocatalytic activity". Mater. Lett. , 112: 90–93, 2013.

[18] Zhang, X.; Su, H.; Yang, X.; "Catalytic performance of a three-dimensionally ordered macroporous Co/ZrO2 catalyst in Fischer–Tropsch synthesis". J. Mol. Catal. A Chem., 360: 16–25, 2012.

[19] Gusmano, G.; Montesperelli, G.; Rapone, M.; Padeletti, G.; Cusmà, A.; Kaciulis, S.; Mezzi, A.; Di. Maggio, R.; "Zirconia primers for corrosion resistant coatings". Surf. Coatings Technol., 201(12): 5822–5828, 2007.

[20] Zhang, C.; Li, C.; Yang, J.; Cheng, Z.; Hou, Z.; Fan, Y.; Lin, J.; "Tunable luminescence in monodisperse zirconia spheres". Langmuir, 25(12): 7078–7083, 2009.

[21] Najibi-Ilkhechi, N.; Koozegar-Kaleji, B.; Salahi, E.; "Effect of heating rate on structural and optical properties of Si and Mg co-doped ZrO _ 2 ZrO 2 nanopowders". Opt. Quantum Electron. 47: 1187–1195, 2015.

[22] Fritzen, D. L.; Giordano, L.; Rodrigues, L. C. V; Monteiro, J. H. S. K.; "Opportunities for persistent luminescent nanoparticles in luminescence imaging of biological systems and photodynamic therapy". Nanomaterials, 10(10): 1-36, 2020.

[23] Zhu, H.; Yang, D.; Xi, Z.; Zhu, L.; "Hydrothermal synthesis and characterization of zirconia nanocrystallites". J. Am. Ceram. Soc., 90(4): pp. 1334–1338, 2007.

[24] Purohit, R. D.; Saha, S.; Tyagi, A. K.; "Combustion synthesis of nanocrystalline ZrO2 powder: XRD, Raman spectroscopy and TEM studies". Mater. Sci. Eng. B, 130(1-3): 57–60, 2006.

[25] Lan, L.; Chen, S.; Cao, Y.; Zhao, M.; Gong, M.; Chen, Y.; "Preparation of ceria–zirconia by modified coprecipitation method and its supported Pd-only three-way catalyst". J. Colloid Interface Sci., 450: 404–416, 2015.

[26] Wang, J. A.; Valenzuela, M. A.; Salmones, J.; Vázquez, A.; Garcıa-Ruiz, A.; Bokhimi, X.; "Comparative study of nanocrystalline zirconia prepared by precipitation and sol–gel methods". Catal. Today, 68(1-3): 21–30, 2001.

[27] Hernandez-Como, N.; Martinez Landeros, V.; Mejia, I.; Aguirre Tostado, F.S.; Nascimento, C.D.; deM.Azevedo, G.; Krug, C. ; Quevedo-Lopez , M.A.; "Defect control in room temperature deposited cadmium sulfide thin films by pulsed laser deposition". Thin Solid Films, 550: 665–668, 2014.

[28] Gokulakrishnan, V.; Parthiban, S.; Jeganathan, K.; Ramamurthi, K.; "Investigation on the effect of Zr doping in ZnO thin films by spray pyrolysis". Appl. Surf. Sci., 257(21): 9068–9072, 2011.

[29] Lee, J.-H.; Song, J. T.; "Dependence of the electrical and optical properties on the bias voltage for ZnO: Al films deposited by rf magnetron sputtering". Thin Solid Films, 516(7): 1377–1381, 2008.

[30] Hussain, J. M.; Jasim, A.S.; Aadim, K. A.; "Synthesis and Characterization of CdOx− 1: MgX films by pulsed laser deposition". Iraqi J. of Physics,18(45): 59-67, 2020.

[31] Mohammed, R. S.; Aadim, K.A.; Ahmed, K.A.; "Synthesis of CuO / ZnO and MgO / ZnO Core / Shell Nanoparticles with Plasma Jets and Study of their Structural and Optical Properties". Karbala Int. J. of Modern Science. 8(2): 213-222. 2022.